

# The matrix stiffness is increased in the eutopic endometrium of adenomyosis patients: a study based on atomic force microscopy and histochemistry

Xiaowen Wang,<sup>1</sup> Wenbin Cai,<sup>2</sup> Ting Liang,<sup>2</sup> Hui Li,<sup>1</sup> Yingjie Gu,<sup>1</sup> Xiaojiao Wei,<sup>1</sup> Hong Zhang,<sup>1</sup> Xiaojun Yang<sup>1</sup>

<sup>1</sup>Department of Obstetrics and Gynecology, The First Affiliated Hospital of Soochow University, Suzhou, Jiangsu Province

<sup>2</sup>Orthopaedic Institute, Medical College, Soochow University, Suzhou, Jiangsu Province, China

## ABSTRACT

Previous ultrasound studies suggest that patients with adenomyosis (AM) exhibit increased uterine cavity stiffness, although direct evidence regarding extracellular matrix (ECM) content and its specific impact on endometrial stiffness remains limited. This study utilized atomic force microscopy to directly measure endometrial stiffness and collagen morphology, enabling a detailed analysis of the endometrium's mechanical properties: through this approach, we established direct evidence of increased endometrial stiffness and fibrosis in patients with AM. Endometrial specimens were also stained with Picrosirius red or Masson's trichrome to quantify fibrosis, and additional analyses assessed  $\alpha$ -SMA and Ki-67 expression. Studies indicate that pathological conditions significantly influence the mechanical properties of endometrial tissue. Specifically, adenomyotic endometrial tissue demonstrates increased stiffness, associated with elevated ECM and fibrosis content, whereas normal endometrial samples are softer with lower ECM content. AM appears to alter both the mechanical and histological characteristics of the eutopic endometrium. Higher ECM content may significantly impact endometrial mechanical properties, potentially contributing to AM-associated decidualization defects and fertility challenges.

**Key words:** adenomyosis; eutopic endometrium; atomic force microscopy; extracellular matrix components; stiffness.

**Correspondence:** Xiaojun Yang, Department of Obstetrics and Gynecology, The First Affiliated Hospital of Soochow University, 188 Shizi Road, Suzhou 215006, Jiangsu Province, China. Tel. +86.18626292163 - Fax: +86.51266919883. E-mail: yang.xiaojun@hotmail.com

**Contributions:** all authors contributed to the study's preparation and design and agree with the content of the manuscript. XW, experimental execution, data collection and analysis, interpretation of results, writing, manuscript revision; WC, TL, AFM detection; HL, YG, XWei, manuscript revision; HZ, specimen acquisition. XY, supervision, review and editing, funding acquisition.

**Conflict of interest:** the authors declare that no conflict of interest.

**Ethics approval:** the experimental protocols were approved by the Medical Ethics Review Board of the First Affiliated Hospital of Soochow University (No. 2024035).

**Funding:** this work was supported by the National Natural Science Foundation of China (grant number: 81971335).

## Introduction

Adenomyosis (AM) is a common gynecological inflammatory disease characterized by the infiltration of endometrial tissue into the myometrium. This condition leads to inflammation and myometrial hypertrophy, presenting clinically with symptoms such as pelvic pain, abnormal uterine bleeding (AUB), and infertility.<sup>1,2</sup> The pathogenesis of AM remains controversial, with primary hypotheses including the endometrial invasion hypothesis,<sup>3</sup> the tissue injury and repair (TIAR)<sup>4</sup> mechanism, and stem cell theory.<sup>5</sup>

Notably, AM is associated with endometrial stromal and epithelial fibrosis. AM exhibits significant increases in platelet aggregation, transforming growth factor (TGF- $\beta$ 1), phosphorylated Smad3, epithelial-to-mesenchymal transition (EMT), and fibroblast-to-myofibroblast transdifferentiation markers. Additionally, smooth muscle metaplasia is increased, along with a rise in fibrosis compared to normal endometrium.<sup>6,7</sup> Evidence from transvaginal elastic ultrasonography<sup>8</sup> indicates that AM lesions are stiffer than fibroids and normal myometrium. However, there is a lack of direct observation or evidence of endometrial fibrosis and stiffness in AM. More importantly, the factors contributing to potentially increased endometrial stiffness remain inconclusive.

Atomic force microscopy (AFM) is a user-friendly, high-resolution technique that can measure mechanical properties at the nanoscale.<sup>9-11</sup> AFM is capable of directly measuring the elastic and viscoelastic properties of biological cells through indentation<sup>12</sup> and has therefore been widely used to characterize the mechanical behavior of cells under healthy and pathological conditions. An increasing number of studies have performed mechanistic characterization of cells in different diseases, including breast cancer,<sup>13,14</sup> bladder cancer<sup>15</sup> and thyroid cancer,<sup>16</sup> to assess cell invasion ability. These studies reveal that malignant cells often exhibit increased deformability, motility, and metastatic potential.

In this study, we used AFM to evaluate the elastic modulus of AM-affected *versus* normal endometrial tissue, providing a direct assessment of disease-induced mechanical changes. This study reports, for the first time, that ECM remodeling and fibrosis occur in the eutopic endometrium of patients with AM, leading to increased endometrial stiffness. We believe that this will inevitably impact reproductive function. We believe that investigating these factors further will deepen our understanding of AM pathology and may aid in developing improved diagnostic, prognostic, and therapeutic strategies for this condition.

## Materials and Methods

### Patients and specimens

Endometrial samples for the AM group (AM, n=6) were collected from women aged 18-45 years with dysmenorrhea who underwent hysterectomy due to AM, suspected by ultrasound and confirmed through postoperative pathology. These women had regular menstrual cycles (24 to 32 days  $\pm$  3 days in length, with a duration of 2-7 days). Endometrial samples for the control group (Ctrl, n=6) were obtained from women of childbearing age (18-45 years) with no history of dysmenorrhea, recurrent miscarriage, or clinical or laparoscopic evidence of AM. Control samples were collected by hysteroscopic biopsy or by sagittal dissection of the uterus after benign hysterectomy using a sterile scalpel. All endometrial samples were taken during the secretory phase of the menstrual cycle. Both groups excluded women with systemic diseases, tumors, endocrine disorders, cardiovascular or rheumatic diseases, or recent hormone therapy (within the past three months).

In this study, "AM" refers to the AM group, and "Ctrl" refers to the normal control group without AM.

Endometrial samples were obtained during surgeries from female subjects. All endometrial samples were collected in accordance with the guidelines of the Declaration of Helsinki and were approved by the Medical Ethics Review Board of the First Affiliated Hospital of Soochow University. Each patient enrolled in this study provided informed consent for all procedures and allowed data collection and analysis for research purposes. The study was non-advertised, and no remuneration was offered to encourage patients to give consent.

### Nanomechanical testing and imaging

One hour after specimen removal, the extracted endometrial tissue was rinsed with PBS, promptly embedded in optimal cutting temperature (OCT) compound, and cryopreserved at -80°C. The frozen tissue block was sectioned into 25  $\mu$ m slices using a cryostat (CM3050 S; Leica, Nussloch, Germany) and temporarily stored at -20°C. Before conducting AFM measurements, each section was immersed in PBS to remove the OCT compound and allowed to thaw at room temperature. Measurements were completed within an hour of thawing to preserve tissue structure. Biomechanical analysis was conducted using an AFM scanner (Dimension ICON, Bruker, Billerica, MA, USA). Figure 1 A,B provides schematic diagrams illustrating the experimental method.

For the microscale experiments, the modulus was determined by employing the force-volume mode within a fluid cell containing 0.15 M PBS (pH 7.4). This was done using a V-shaped silicon nitride cantilever with an affixed borosilicate glass sphere of 5  $\mu$ m in diameter. The spherical tip, with a spring constant of 0.06 N/m (Bruker), was utilized. The calculation of the elastic modulus involved the following equation:

$$E = \frac{\sqrt{\pi}}{2} (1 - \nu^2) \frac{S}{\sqrt{A}}$$

where E is the elastic modulus, Poisson's ratio ( $\nu$ ), S represents the contact stiffness (the slope observed in the initial section of the unloading regime of the load-indentation curve), and A corresponds to an area function linked to the effective cross-sectional, or projecting area, of the indenter, as described in previous studies. The detailed calculation methodology can be found in earlier investigations.<sup>17, 18</sup> For nanoscale experiments, images of collagen fibers were obtained using a ScanAsyst-Air probe with a radius of curvature of 5 nm and a force constant of 0.4 N/m. NanoScope analysis software (Bruker) was used to obtain relevant information about fibrils through line cross-section analysis, including arrangement, diameter, and other characteristics. Figure 2D illustrates the experimental method with a schematic diagram.

### Evaluation with histology

To further assess the extent of endometrial fibrosis, endometrial specimens were fixed in 4% paraformaldehyde, embedded in paraffin, dewaxed, rehydrated in distilled water, and stained with hematoxylin and eosin (HE), Picrosirius red (PSR) or Masson's trichrome (MTC), using staining kits (PSR: Servicebio, Wuhan, China; G1018; MTC: Servicebio, G1006) according to the manufacturer's instructions. PSR and MTC staining were used to detect collagen fibrils deposited within the matrix.<sup>19</sup> To objectively quantify the extent of fibrosis in the endometrium stained for collagen with PSR or MTC, we used ImageJ version 1.53q (National Institutes of Health, Bethesda, MD). For each specimen, six random fields of view were analyzed at 40x magnification. Fiber content was quantified as a percentage of the total positive staining

area. In PSR staining, positive results appear as red collagen fibers, while in MTC staining, positive staining appears as blue collagen fibers.

### Immunohistochemistry and immunofluorescence

For Ki-67 immunohistochemical analysis, 4  $\mu\text{m}$  paraffin-embedded tissue sections were prepared, dewaxed, and subjected to antigen retrieval. The sections were placed in a repair box containing citric acid antigen retrieval buffer (Phyngnen, PH0422) and heated in a microwave. The temperature was maintained at medium heat for 8 min until boiling, followed by medium-low heat for 7 min. After natural cooling, the slides were placed in PBS (pH 7.4) and washed three times on a decolorizing shaker, each wash lasting 5 min. Endogenous peroxidase activity was quenched by treating sections with 3% hydrogen peroxide in phosphate-buffered saline (PBS) for 25 min at room temperature in the dark. Subsequently, sections were blocked with 3% bovine serum albumin (Servicebio, GC305010) for 30 min at room temperature. After washing with PBS (pH 7.4), sections were incubated overnight at 4°C with primary antibodies: anti-Ki-67 mouse antibody (Servicebio, GB121141) diluted 1:500. In the negative control group, tissues were incubated with PBS only, without the anti-Ki-67 primary antibody. The secondary antibody used was HRP-conjugated goat anti-mouse IgG (Servicebio, GB23301) diluted 1:200, and sections were incubated for 50 min at room temperature. Subsequently, DAB chromogenic solution (Servicebio, G1212) was used to develop the color, and the cell nuclei were counterstained with hematoxylin. To quantify Ki-67-labeled cells, we calculated the percentage of labeled cells relative to the total number of hematoxylin-stained nuclei. For each sample, six randomly selected fields at 40 $\times$  magnification were counted under a Nikon Eclipse C1 upright fluorescence microscope. The average percentage of labeled cells was then calculated for each sample.

For immunofluorescence, primary antibodies included mouse anti- $\alpha$ -SMA antibody (Servicebio, GB12044) at a 1:500 dilution. Tissue sections were blocked with 3% bovine serum albumin (Servicebio, GC305010) for 30 min and then washed with PBS (pH 7.4). Slides were then incubated with primary antibodies overnight at 4°C and washed in buffer. Further incubations included secondary antibodies: Alexa Fluor<sup>®</sup> 488-conjugated goat anti-mouse IgG (Servicebio, GB25301) at a 1:400 dilution and CY3-conjugated goat anti-rabbit IgG (Servicebio, GB21303) at a 1:300 dilution. After washing, DAPI staining solution (Servicebio, G1012) was added for nuclear counterstaining. Finally, the slides were sealed with anti-fluorescence quenching mounting medium (Servicebio, G1401) and used with Nikon Eclipse C1 upright fluorescence equipped with oil immersion and a 40x objective. Observations were performed microscopically. To quantify  $\alpha$ -SMA labeled cells, we reported the percentage of labeled cells relative to the total number of DAPI-stained nuclei. For each sample, six fields at 40x magnification were randomly selected and counted. The average percentage of labeled cells was calculated for each sample.

### Statistical analysis

All data are presented as mean  $\pm$ SEM and were analyzed using GraphPad Prism version 10.0.1. After confirming normal distribution and homogeneity of variances using the Shapiro-Wilk test and Bartlett's test, the Student's *t*-test was used for analysis. Statistical significance was determined at  $p < 0.05$ .

## Results

### Increased endometrium stiffness in patients with adenomyosis

Figure 2A shows the results of endometrial stiffness measurements (Young's modulus). For the first time, we report changes in the mechanical microenvironment of the eutopic endometrium in patients with AM. The study found that the Young's modulus of the AM group ( $21.21 \pm 1.628$  kPa) was significantly higher than that of the control group ( $4.726 \pm 0.3845$  kPa). Since tissue stiffness and collagen distribution are closely related, we investigated collagen arrangement or distribution in the endometrium of both groups to further explore the potential contributors to the increased tissue stiffness. In the control group, as shown in Figure 2B (a-d), the normal arrangement of collagen fibers can be clearly observed,

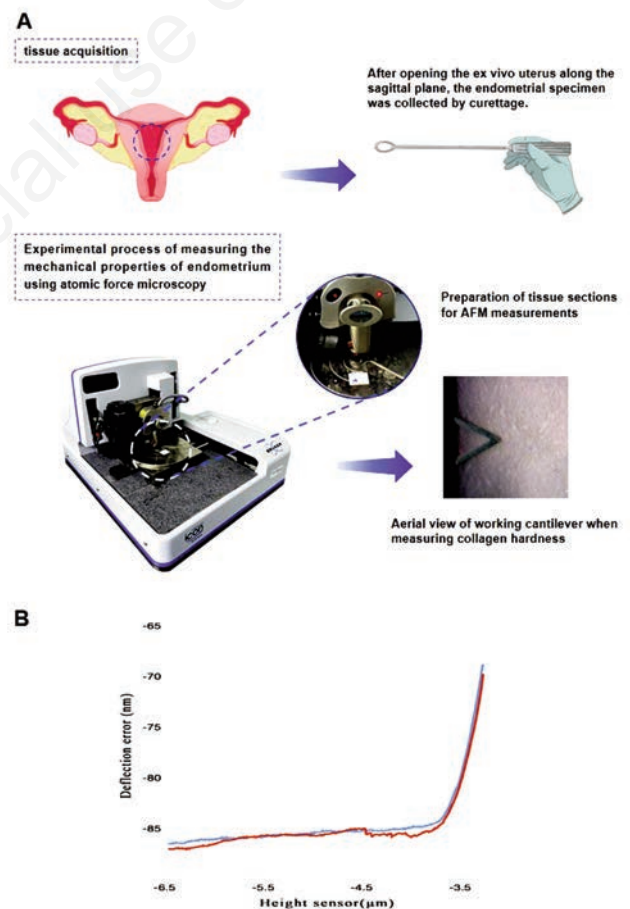


**Figure 1.** Illustration of the process for measuring endometrial stiffness using AFM. **A)** Schematic diagram of the process for detecting endometrial stiffness with AFM. **B)** Data obtained from AFM measurements. The AFM tip applies force to the tissue, and the indentation depth ( $\mu\text{m}$ ) and deflection error (nm) are recorded. These results are used to calculate elasticity using a standard calculation.

which is an elongated chain-like structure with relatively consistent thickness, an orderly arrangement, and no cross-linking between fibers. In contrast, the arrangement of collagen structures in the disease group shown in Figure 2B (e–h) appeared more disordered and cross-linked. Meanwhile, Figure 2C shows the results of the collagen diameter measured in both groups of eutopic endometrium. No significant difference in collagen diameter was observed between the AM group ( $92.57 \pm 3.016$  nm) and the control group ( $85.71 \pm 2.718$  nm).

### Increased endometrium fibrosis in AM

To investigate the reasons behind the endometrial sclerosis, we stained the specimens to investigate the degree of fibrosis. The degree of endometrial fibrosis was assessed using HE, PSR, or MTC. Figure 3A shows representative photomicrographs of the endometrium. Figure 3 B,C shows the percentage of the positive area for PSR and MTC, respectively, indicating significant higher proportion of positive staining in the eutopic endometrium of patients with AM than the control. A higher percentage of positively stained areas indicates an increase in the degree of fibrosis.

### Increased endometrium $\alpha$ -SMA expression in AM

To investigate the contributors of fibrosis in AM, we examined the expression of  $\alpha$ -SMA, a marker of myofibroblasts and smooth muscle cells, as increased  $\alpha$ -SMA expression typically indicates myofibroblast formation. Figure 4A is the representative images of  $\alpha$ -SMA-positive fluorescent staining. As shown in Figure 4B, the proportion of positive  $\alpha$ -SMA staining in the eutopic endometrium of patients with AM ( $40.82 \pm 1.253\%$ ) is significantly higher than that in the control group ( $13.72 \pm 0.9102\%$ ), suggesting ECM remodeling in AM.

### Enhanced cell proliferation in the stromal zone of the endometrium in AM

Ki-67, a well-established marker for evaluating cell proliferation in both benign and malignant diseases, was used to assess cellular proliferation activity in the epithelial and stromal regions.<sup>20,21</sup> Figure 5 A,B shows that in the control group, Ki-67-positive cells were primarily located in the epithelial area ( $1.062 \pm 0.1304\%$ ), indicating normal proliferative activity within the epithelium. In contrast, the disease-affected group exhibited a significantly higher

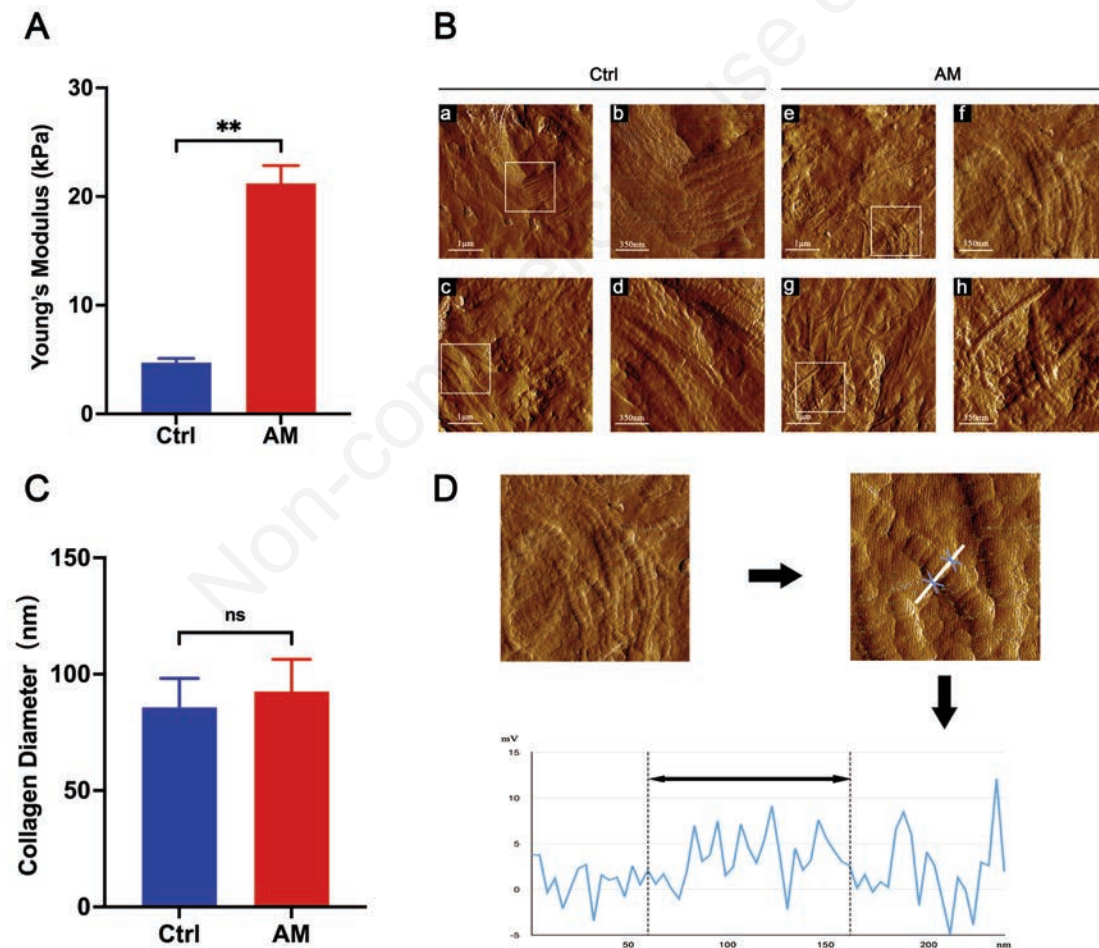


**Figure 2.** Illustration of the process of measuring endometrial stiffness and collagen diameter using AFM. **A)** Statistical chart of endometrial stiffness value (Young's modulus);  $**p < 0.01$ . **B)** Typical image of collagen fibers in the endometrium; (a–d) collagen fibers in the control group; (e–h) collagen fibers in the AM group; the framed area in the image represents a typical collagen fiber arrangement, with the corresponding enlarged image shown on the right. **C)** Bar graph of collagen diameter (nm) in the endometrium from control and AM groups; data are expressed as mean  $\pm$  SEM; ns,  $p \geq 0.05$ . **D)** The diameter of the fibrils was obtained by line section analysis using NanoScope analysis software (Bruker); double-sided arrows show the measured length of one collagen diameter.

proportion of Ki-67-positive cells in the stromal area ( $3.387 \pm 0.5702\%$ ), reflecting increased stromal cell proliferation associated with AM.

## Discussion

Many issues in biomedicine cannot be fully explained by biochemical mechanisms alone, as they are closely intertwined with mechanical processes.<sup>22-24</sup> Mechanomics and biomechanics provide new perspectives on numerous medical challenges, and underscore the importance of understanding mechanical properties for the diagnosis and treatment of uterine diseases. Unlike elastography techniques, such as ultrasound and magnetic resonance elastography which also focused on the mechanics of tissues, AFM allows for localized and whole-cell studies of cellular mechanical properties in their natural environment.<sup>25,26</sup> It provides detailed insights into morphological structures (*e.g.*, height, surface roughness, fiber orientation) and mechanical characteristics (*e.g.*, Young's modulus, stiffness, adhesion energy, adhesion force, tension).<sup>27</sup> This method uniquely offers high-resolution structural, mechanical, and functional information, making AFM a promising

tool for disease research, diagnosis, and monitoring, and potentially filling an important gap in current clinical diagnostics.<sup>28-30</sup>

Research has revealed that the endometrium in patients with AM differs from the one in individuals without this condition, showing multiple metabolic and molecular abnormalities.<sup>4,31,32</sup> This leads to increased angiogenesis and cellular proliferation, decreased apoptosis, progesterone resistance, and altered cytokine expression, resulting in an abnormal immune response and reduced reproductive performance.<sup>33</sup> Under physiological conditions, the endometrial ECM stiffness changes during embryo implantation, aiding cell movement.<sup>34,35</sup> Moreover, changes in endometrial stiffness in AM patients impact pregnancy outcomes by affecting trophoblast adhesion and invasion.<sup>36</sup> A stiffer endometrial matrix can hinder embryonic invasion and placental function, potentially leading to late miscarriage and premature delivery. Understanding these factors is crucial in managing AM-related fertility issues.

Biological tissue mechanics vary significantly under different physiological and pathological conditions, as cells remodel ECM in response to disease. This remodeling often involves changes in ECM synthesis and regulation by cells. Currently, limited research exists on the mechanical properties of human endometrial tissue. Alterations in the components of the endometrial ECM can directly impact mechanical properties, such as tissue stiffness. Collagen, the

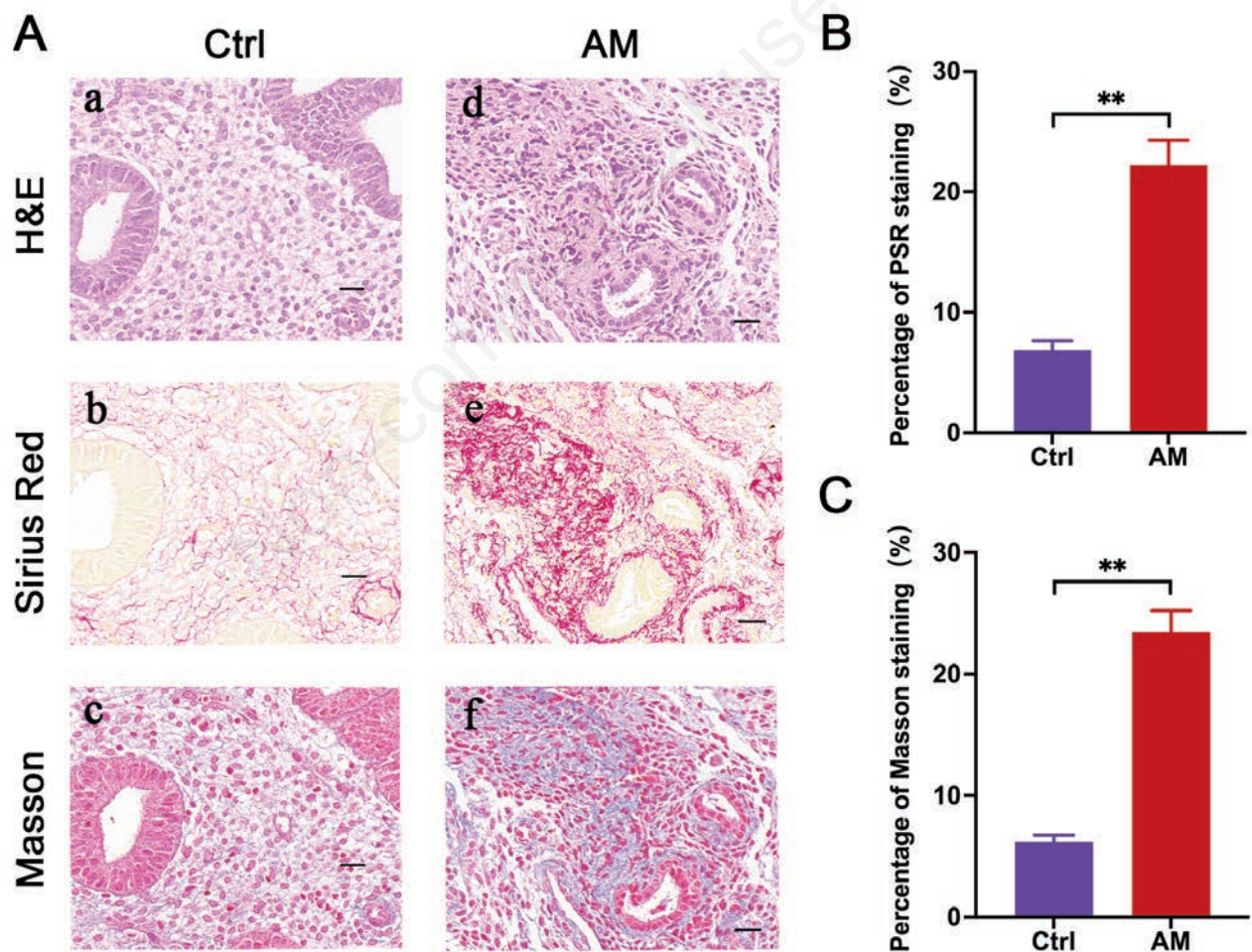


**Figure 3.** Effect of AM on eutopic endometrial fibrosis. **A)** Representative photomicrographs of the eutopic endometrium stained with HE, PSR, or MTC; (a-c) staining of the control group; (d-f) staining of the AM group; scale bars: 20  $\mu\text{m}$ . **B)** The positive area of PSR staining significantly increased in patients with AM;  $**p < 0.01$ . **C)** The positive area of MTC staining significantly increased in patients with AM;  $**p < 0.01$ .

most abundant ECM protein, contributes significantly to the tensile strength and stiffness of tissue.<sup>37</sup> Other studies have also confirmed that cross-linking between collagen and elastin molecules can increase fiber stiffness.<sup>38-40</sup> This study observed similarly increased collagen cross-linking in the eutopic endometrium of patients with AM, contributing to increased endometrial stiffness. Notably, collagen fiber diameter showed no significant difference between AM and normal endometrial tissue, aligning with findings by Zakaria *et al.* in lung cancer tissue, where increased collagen concentration and density did not alter fiber diameter.<sup>41</sup> This suggests that fiber diameter alone does not determine tissue stiffness; rather, stiffness likely results from the cumulative effects of ECM components,<sup>42</sup> particularly the excessive synthesis and deposition of ECM proteins.<sup>30</sup>  $\alpha$ -SMA, an actin isoform crucial to fibrogenesis, is highly expressed in AM, where its upregulation is associated with fibroblast subtypes possessing strong ECM remodeling capabilities, correlating with the

increased stiffness observed *in situ*.<sup>43</sup> Additionally,  $\alpha$ -SMA is linked to the activation of mechanosensitive signaling pathways: filamentous  $\alpha$ -SMA activates mitogen-activated protein kinase (MAPK) signaling, and cells overexpressing  $\alpha$ -SMA exhibit tension-induced enhancement of p38 activation.<sup>44</sup> However, whether this pathway is involved in endometrial fibrosis in AM remains unclear, warranting further research. Moreover, Ki-67 staining indicates dominant stromal cell proliferation in AM, though it is uncertain if this is driven by EMT, which could confer migratory and invasive properties to cells, leading to stromal cell migration and proliferation. On the other hand, endometrial stromal cells from patients with endometriosis can move through small channels quickly, showing high flexibility and lower stiffness.<sup>45</sup> This could explain their abnormal movement and invasiveness. These findings highlight the importance of understanding tissue mechanics in conditions like AM for future research on cell-ECM interactions in endometrial tissue.

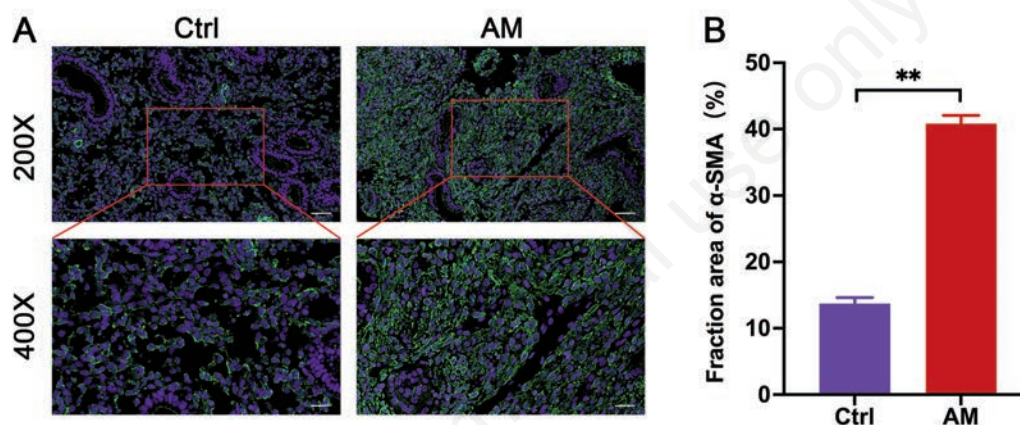


**Figure 4.** Immunofluorescence staining of  $\alpha$ -SMA in the endometrial tissue of both groups. **A)** Expression of  $\alpha$ -SMA; upper magnification 200x scale bar: 50  $\mu$ m; lower magnification 400x, scale bar: 25  $\mu$ m. **B)** The proportion of  $\alpha$ -SMA-positive staining area is higher in the AM group compared to the normal control group; \*\* $p < 0.01$ .

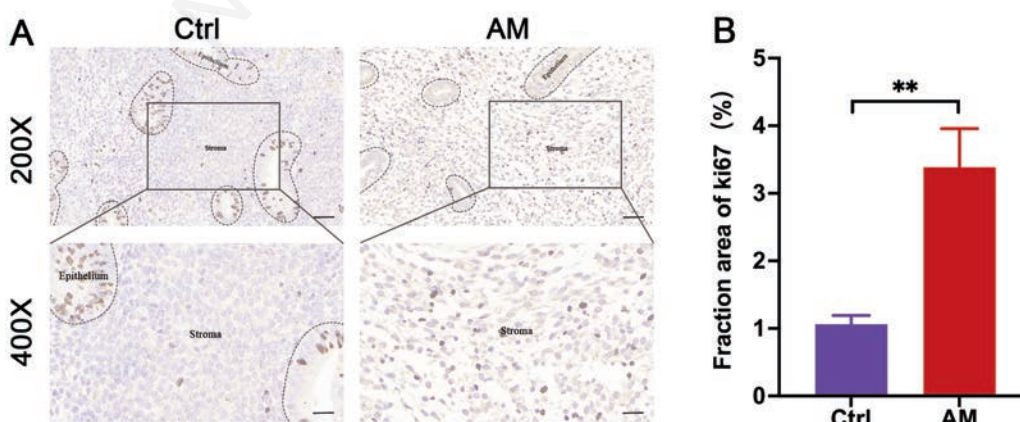


**Figure 5.** Immunohistochemical staining of Ki-67 in the endometrial tissue of both groups. **A)** Ki-67 positivity was primarily localized in the epithelial region in the control group, whereas it was more pronounced in the stromal region in the AM group; upper magnification 200x scale bar: 50  $\mu$ m; lower magnification 400x, scale bar: 25  $\mu$ m. **B)** Quantitative analysis showed significantly higher Ki-67 positivity, indicating overactive stromal cell proliferation, in the AM group compared to the normal epithelium in the control group; \*\* $p < 0.01$ .

## Acknowledgements

The authors greatly appreciate the excellent support and assistance provided by the Central Research Laboratory at the First Affiliated Hospital of Soochow University for this work.

## References

- Vannuccini S, Tosti C, Carmona F, Huang SJ, Chapron C, Guo S-W, et al. Pathogenesis of adenomyosis: an update on molecular mechanisms. *Reprod Biomed Online* 2017;35:592-601.
- Vannuccini S, Petraglia F. Recent advances in understanding and managing adenomyosis. *F1000Res* 2019;8:283-92.
- Bergeron C, Amant F, Ferenczy A. Pathology and physiopathology of adenomyosis. *Best Pract Res Clin Obstet Gynaecol* 2006;20:511-21.
- Benagiano G, Habiba M, Brosens I. The pathophysiology of uterine adenomyosis: an update. *Fertil Steril* 2012;98:572-9.
- Hufnagel D, Li F, Cosar E, Krikun G, Taylor HS. The role of stem cells in the etiology and pathophysiology of endometriosis. *Semin Reprod Med* 2015;33:333-40.
- Liu X, Shen M, Qi Q, Zhang H, Guo S-W. Corroborating evidence for platelet-induced epithelial-mesenchymal transition and fibroblast-to-myofibroblast transdifferentiation in the development of adenomyosis. *Hum Reprod* 2016;31:734-49.
- Shen M, Liu X, Zhang H, Guo S-W. Transforming growth factor  $\beta$ 1 signaling coincides with epithelial-mesenchymal transition and fibroblast-to-myofibroblast transdifferentiation in the development of adenomyosis in mice. *Hum Reprod* 2016;31:355-69.
- Liu X, Ding D, Ren Y, Guo S-W. Transvaginal elastosonography as an imaging technique for diagnosing adenomyosis. *Reprod Sci* 2018;25:498-514.
- Gadegaard N. Atomic force microscopy in biology: technology and techniques. *Biotech Histochem* 2006;81:87-97.
- Allison DP, Mortensen NP, Sullivan CJ, Doktycz MJ. Atomic force microscopy of biological samples. *Wiley Interdiscip Rev Nanomed Nanobiotechnol* 2010;2:618-34.
- Stylianou A, Kontomaris S-V, Grant C, Alexandratou E. Atomic force microscopy on biological materials related to pathological conditions. *Scanning* 2019;2019:8452851.
- Darling EM, Topel M, Zauscher S, Vail TP, Guilak F. Viscoelastic properties of human mesenchymally-derived stem cells and primary osteoblasts, chondrocytes, and adipocytes. *J Biomech* 2008;41:454-64.
- Jiang X, Asbach P, Streitberger K-J, Thomas A, Hamm B, Braun J, et al. In vivo high-resolution magnetic resonance elastography of the uterine corpus and cervix. *Eur Radiol* 2014;24:3025-33.
- Li QS, Lee GYH, Ong CN, Lim CT. AFM indentation study of breast cancer cells. *Biochem Biophys Res Commun* 2008;374:609-13.
- Canetta E, Riches A, Borger E, Herrington S, Dholakia K, Adya AK. Discrimination of bladder cancer cells from normal urothelial cells with high specificity and sensitivity: combined application of atomic force microscopy and modulated Raman spectroscopy. *Acta Biomater* 2014;10:2043-55.
- Prabhune M, Belge G, Dotzauer A, Bullerdiel J, Radmacher M. Comparison of mechanical properties of normal and malignant thyroid cells. *Micron* 2012;43:1267-72.
- Stolz M, Raiteri R, Daniels AU, VanLandingham MR, Baschong W, Aebi U. Dynamic elastic modulus of porcine articular cartilage determined at two different levels of tissue organization by indentation-type atomic force microscopy. *Biophys J* 2004;86:3269-83.
- Liang T, Che Y-J, Chen X, Li H-T, Yang H-L, Luo Z-P. Nano and micro biomechanical alterations of annulus fibrosus after in situ immobilization revealed by atomic force microscopy. *J Orthop Res* 2019;37:232-8.
- Zuo F, Kaminski N, Eugui E, Allard J, Yakhini Z, Ben-Dor A, et al. Gene expression analysis reveals matrilysin as a key regulator of pulmonary fibrosis in mice and humans. *Proc Natl Acad Sci USA* 2002;99:6292-7.
- Alonso-Magdalena P, Brössner C, Reiner A, Cheng G, Sugiyama N, Warner M, et al. A role for epithelial-mesenchymal transition in the etiology of benign prostatic hyperplasia. *Proc Natl Acad Sci USA* 2009;106:2859-63.
- Pathmanathan N, Balleine RL. Ki67 and proliferation in breast cancer. *J Clin Pathol* 2013;66:512-6.
- Bao G, Suresh S. Cell and molecular mechanics of biological materials. *Nat Mater* 2003;2:715-25.
- Darling EM, Di Carlo D. High-throughput assessment of cellular mechanical properties. *Annu Rev Biomed Eng* 2015;17:35-62.
- Pettenuzzo S, Arduino A, Belluzzi E, Pozzuoli A, Fontanella CG, Ruggieri P, et al. Biomechanics of chondrocytes and chondrons in healthy conditions and osteoarthritis: a review of the mechanical characterisations at the microscale. *Biomedicines* 2023;11:1942.
- Charras GT, Horton MA. Single cell mechanotransduction and its modulation analyzed by atomic force microscope indentation. *Biophys J* 2002;82:2970-81.
- Trache A, Meininger GA. Atomic force microscopy (AFM). *Curr Protoc Microbiol* 2008;Chapter 2:Unit 2C.2.
- Liu S, Han Y, Kong L, Wang G, Ye Z. Atomic force microscopy in disease-related studies: Exploring tissue and cell mechanics. *Microsc Res Tech* 2024;87:660-84.
- Guolla L, Bertrand M, Haase K, Pelling AE. Force transduction and strain dynamics in actin stress fibres in response to nanonewton forces. *J Cell Sci* 2012;125:603-13.
- Haase K, Pelling AE. Investigating cell mechanics with atomic force microscopy. *J R Soc Interface* 2015;12:20140970.
- Kurek A, Kłosowicz E, Sofińska K, Jach R, Barbasz J. Methods for studying endometrial pathology and the potential of atomic force microscopy in the research of endometrium. *Cells* 2021;10:219-36.
- Carvalho L, Podgac S, Bellodi-Privato M, Falcone T, Abrão MS. Role of eutopic endometrium in pelvic endometriosis. *J Minim Invasive Gynecol* 2011;18:419-27.
- Brosens I, Brosens JJ, Benagiano G. The eutopic endometrium in endometriosis: are the changes of clinical significance? *Reprod Biomed Online* 2012;24:496-502.
- Ota H, Igarashi S, Hatazawa J, Tanaka T. Is adenomyosis an immune disease? *Hum Reprod Update* 1998;4:360-7.
- Ruiz LA, Báez-Vega PM, Ruiz A, Peterse DP, Monteiro JB, Bracero N, et al. Dysregulation of lysyl oxidase expression in lesions and endometrium of women with endometriosis. *Reprod Sci.* 2015;22:1496-508.
- Grewal S, Carver JG, Ridley AJ, Mardon HJ. Implantation of the human embryo requires Rac1-dependent endometrial stromal cell migration. *Proc Natl Acad Sci USA* 2008;105:16189-94.
- Cao J, Li H, Tang H, Gu X, Wang Y, Guan D, et al. Stiff extracellular matrix promotes invasive behaviors of trophoblast cells. *Bioengineering (Basel)* 2023;10:384-97.
- Koláčná L, Bakesová J, Varga F, Kostáková E, Plánka L, Necas A, et al. Biochemical and biophysical aspects of collagen nanostructure in the extracellular matrix. *Physiol Res*

- 2007;56:S51-S60.
38. Xiao Q, Ge G. Lysyl oxidase, extracellular matrix remodeling and cancer metastasis. *Cancer Microenviron* 2012;5:261-73.
39. Bailey AJ. Molecular mechanisms of ageing in connective tissues. *Mech Ageing Dev* 2001;122:735-55.
40. Miles CA, Avery NC, Rodin VV, Bailey AJ. The increase in denaturation temperature following cross-linking of collagen is caused by dehydration of the fibres. *J Mol Biol* 2005;346:551-6.
41. Zakaria MA, Aziz J, Rajab NF, Chua EW, Masre SF. Tissue rigidity increased during carcinogenesis of NTCU-induced lung squamous cell carcinoma in vivo. *Biomedicines* 2022;10:238-50.
42. Achilli M, Mantovani D. Tailoring mechanical properties of collagen-based scaffolds for vascular tissue engineering: the effects of pH, temperature and ionic strength on gelation. *Polymers* 2010;2:664-80.
43. Arora PD, McCulloch CA. Dependence of collagen remodeling on alpha-smooth muscle actin expression by fibroblasts. *J Cell Physiol* 1994;159:161-75.
44. Wang J, Fan J, Laschinger C, Arora PD, Kapus A, Seth A, et al. Smooth muscle actin determines mechanical force-induced p38 activation. *J Biol Chem* 2005;280:7273-84.
45. Altayyeb A, Othman E, Khashbah M, Esmael A, El-Mokhtar M, Lambalk C, et al. Characterization of mechanical signature of eutopic endometrial stromal cells of endometriosis patients. *Reprod Sci* 2020;27:364-74.

Non-commercial use only

---

Received: 15 August 2024. Accepted: 18 November 2024.

This work is licensed under a Creative Commons Attribution-NonCommercial 4.0 International License (CC BY-NC 4.0).

©Copyright: the Author(s), 2024

Licensee PAGEPress, Italy

*European Journal of Histochemistry* 2024; 68:4131

doi:10.4081/ejh.2024.4131

*Publisher's note: all claims expressed in this article are solely those of the authors and do not necessarily represent those of their affiliated organizations, or those of the publisher, the editors and the reviewers. Any product that may be evaluated in this article or claim that may be made by its manufacturer is not guaranteed or endorsed by the publisher.*